1 Preparation

1.1 Theoretical Background

1.1.1 γ-Radiation and Decay

There are different kinds of radiation. In the experiments there are EM-radiation, α-radiation, β^+- and β^--radiation as well as radiation of neutrons. Important for compton scattering is the γ-radiation, a part of the electro magnetic spectrum.
It is emitted when atoms decay and the new atom is in an excited state. Photons are emitted as the atom relaxes to the ground state.
The γ-radiation can be expanded in multipoles, i.e. a sum of spherical harmonics. The parity of the L-th multipole is$(-1)^L$. Induced by the decay the electric and magnetic part has the parity $(-1)^L$ resp. $(-1)^{L+1}$. Hence, the order of the magnetic part is higher by 1 than the electric, so that mainly the electric part is observed.
The standard rule to add two angular momentums in QM gives for the initial state J_i and the final state J_f of the relaxing atom:

$$|J_f - J_i| \leq L \leq |J_f + J_i|$$

1.1.2 Interaction of Photons with Matter

There are different effects that play a role when photons interact with matter. Which effect is dominant depends on the energy of the photon as well as the atomic number Z. All effects have in common that the photon is either absorbed or scattered, so that there are less photons after the interaction with matter in the initial direction. The intensity follows an exponential law:

$$I(d) = I(0) \cdot e^{-\mu \cdot d}$$

Compton scattering dominantes starting at about 100 keV up to 10 MeV.
Photons with the energy E are scattered inelasticly with a charged particle with the energy E_0. The photon loses some energy and changes its direction, the electron's kinetic energy increases. Conservation of 4-momentum gives the energy of the scattered photon as a function of the initial energy E and the polar angle Θ:

$$E' = \frac{E}{1 + \frac{E}{E_0} \cdot (1 - \cos\Theta)}$$

1.1.3 Cross Section

The cross section σ gives the probability of a particle to interact with a target. Referring to some statics it is defined as:

$$\sigma = \frac{N_{int} \cdot F}{N_{all} \cdot N_{targets}}$$

with the number of interacting particles N_{int}, the cross section the beam F, the total number of particles in the beam N_{all} and the number of targets $N_{targets}$. It has the same unit as a plane and is often visualized as such. In fact the cross section of two colliding billiard balls is just there geometric cross section. In other cases the cross section decreases with the distance of the two objects, e.g. Rutherford Scattering which depends on the electromagnetic interaction.
The differential cross section with respect to the solid angle Ω is often used and it is assumed to be independent of the azimuthal angle Φ.
There is a theoretical formula by Klein and Nishina for the cross section of compton scattering.

1.1.4 Experimental Setup

Monoenergetic γ-radiation is emitted by a ^{137}Cs source. The target is a Al-Cylinder. The detector is made of NaJ and can be moved on a circle around the target.
We will measure the energy and the number of the photons after the scattering as a function of the polar angle Θ. This is because we assume rotational symmetry.

1.1.5 Assignment 1

We meassure the differential cross section with respect to the solid angle. For this the detector measures the number of incoming photons. For evaluating we use following formula:

$$\frac{d\sigma}{d\Omega} = \frac{R(\Delta\Omega)}{\Delta\Omega} \cdot \frac{1}{\Phi_0 n} \cdot \frac{1}{\epsilon}$$

In this formula $\frac{R(\Delta\Omega)}{\Delta\Omega}$ is a approximation of detector surface because it is not a small dot. $R(\Delta\Omega)$ is the photon stream, the number of detected photons per time interval. We also devide by Φ_0 the incoming photon stream. $\frac{1}{\epsilon}$ is a given number to desribe the not detected electrons and finally n is the number of electrons in the target, which follows from the cylindric geometry, the desity and the atomic number:

$$n = \frac{L}{A} \cdot Z\rho\pi(\frac{d}{2})^2 \cdot l$$

1.1.6 Assignment 2

In assignment 2 we meassure the energy of the photons after the scattering as a function of the angle Θ and the initial energy.
First, we must calibrate the system with known sources. Then we make the meassurement and use the formula above in a slightly different way. A linear regression gives us the invariant mass of electrons.

$$\frac{1}{E'} = \frac{1}{E} + \frac{1}{m_0 \cdot c^2} \cdot (1 - \cos\Theta)$$

1.1.7 Assignment 3

The above formula gives the differential cross section for a single electron. For the whole atom it should be proportional to the atomic number, given that the photon energy is large with respect to the binding energy. With this assumption and the above equations from assignment we can write

$$(\frac{\mathrm{d}\sigma}{\mathrm{d}\Omega})_e = const. \cdot R\frac{A}{\rho Z}$$

2 Evaluation

2.1 Calibration

First we have to calibrate the system. We only measure the number of entries in different channels, but we know at which energies the spectrum of ^{22}Na, ^{60}Co and ^{137}Cs have peaks due to radiation. With these values we can make a linear regression and map the channels onto energies.
Fig.2.1 shows the entries in each channel for ^{22}Na as an example. We fitted the peaks with gaussian functions to get better estimated values.
In Fig.2.2 you can see the channels of each peak and the corresponding energies.
Fig.2.3 finally shows the linear regression with the following parameters:

$$\mathrm{y-intercept} = (-3.02810 \pm 1.48205) \cdot 10^2 \ keV$$

$$\mathrm{slope} = (3.64232 \pm 0.513385) \ keV$$

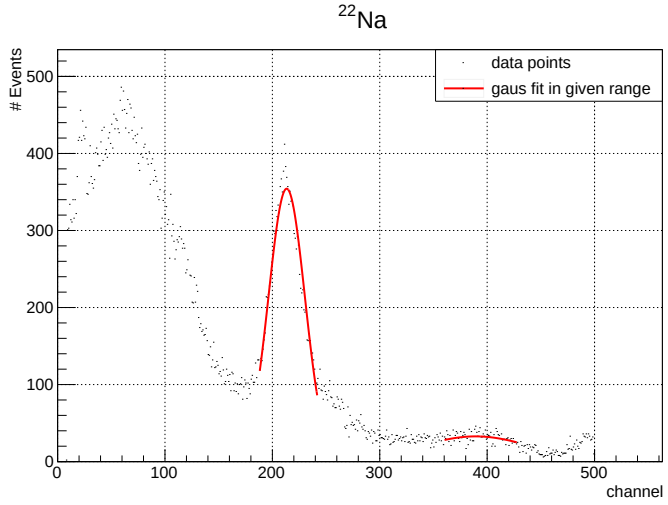

Figure 2.1: Measured channels for ^{22}Na. At estimated ranges we fitted gaussian distributions to get better estimates of the peaks.

Figure 2.2: Measured channels and corresponding energies. Data for a linear fit.

	mean	sigma	energy in keV
^{22}Na	213.33	16.88	511.0
^{22}Na	389.31	52.35	1274.6
^{60}Co	362.87	68.07	1173.2
^{60}Co	463.79	32.98	1332.6
^{137}Cs	278.01	16.78	661.7

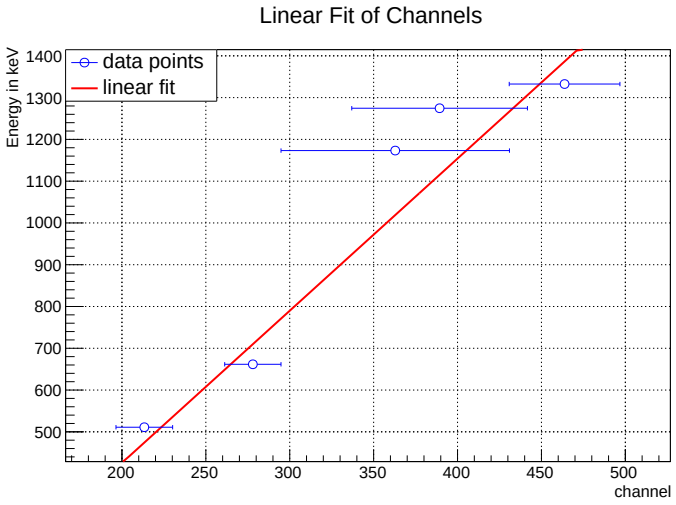

Figure 2.3: Linear fit of channels and corresponding energies. The slope and intersection make it possible so that we can map the channels on the energies.

2.2 Differential Cross Section

Next we measure the diffential cross section with respect to the solid angle Ω. We assume that it has a rotation symmetry, i.e. it is independend of the azimuth ϕ.
We change the angle in $10°$ steps ranging from $20°$ to $100°$ and measure the background without target and the events with target. The sum of the difference is the total number scattered R.
To calculate the cross section we use the formular given in corresponding part of the preparation.

$$\frac{d\sigma}{d\Omega} = \frac{R(\Delta\Omega)}{\Delta\Omega} \cdot \frac{1}{\Phi_0 n} \cdot \frac{1}{\epsilon}$$

To mention is the decay of the source, so we had to correct it by a factor $2^{-t/t_{1/2}}$ with $t_{1/2} = 30a$ and $t = 2016 - 1971 = 45a$. We also multiplied this value by the time we measured the events $t_{meassurement} = 300s$
The values used are the following:

$$\Delta\Omega = \pi \cdot (d/2)^2 / r^2_{target-crystal} = 1.10 \cdot 10^{-2}$$

$$n = \frac{L}{A} \cdot Z\rho\pi(\frac{d}{2})^2 \cdot l = 6.15 \cdot 10^{23}$$

$$\Phi_0 = (1.54 \pm 0.09) \cdot 10^6 \mathrm{cm}^{-2}\mathrm{s}^{-1}$$

$$\frac{1}{\epsilon} = 2.08 \pm 0.01$$

Fig.2.5 shows the values of the polar angle Θ, the measured cross section with its errors and the theoretical values from Klein-Nishina-Formular. These values are plotted in Fig.2.4. For bigger angles Θ, the difference is bigger.

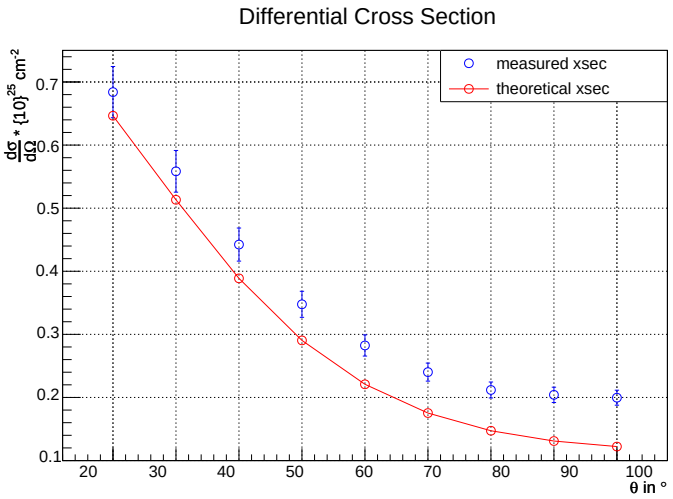

Figure 2.4: Measured and theoretical Cross section.

Figure 2.5: Angles Θ and the measured differential cross section in $10^{25} \cdot cm^2$.

Θ in $^\circ$	$\frac{d\sigma}{d\Omega}$ in $10^{25} \cdot cm^2$	error in $10^{25} \cdot cm^2$	theoretical value in $10^{25} \cdot cm^2$
20	0.684	0.041	0.646
30	0.558	0.033	0.513
40	0.442	0.026	0.389
50	0.348	0.021	0.290
60	0.282	0.017	0.221
70	0.240	0.014	0.175
80	0.212	0.013	0.147
90	0.204	0.012	0.131
100	0.200	0.012	0.122

2.3 Energy Shift and Invariant Mass of Electrons

The energy of a fixed angle is determined by a gaussian fit, an example is shown in Fig.2.6 for $\Theta = 50°$. The procedure is the same as in the calibration subsection above. Using the measured linear fit from above we can acquire the energies given the channels.
Using the results calculated in the calibration and using the deviation of the gaus distributions for the channel error we find the energy:

$$E = (-302.81 + 3.64 \cdot \text{channel})\ keV$$

$$\sigma_E^2 = (148.21^2 + \text{channel}^2 \cdot 0.51^2 + 3.64^2 \cdot \sigma_{channel}^2)\ keV$$

In the equation for the error you can see that there is a part, $(148.21\ keV)^2$, which does not depend on the channel or the deviation of it. This originates from the y-intersect of the calibration fit. For small channel numbers and small errors of the channel number, this becomes the dominating part. The result is a big relative uncertainty for big values of the inverse energy $\frac{1}{E}$, which is the reason for the appereance of the graph below. The fit results and the corresponding energies for each angle Θ are given in Fig.2.7.

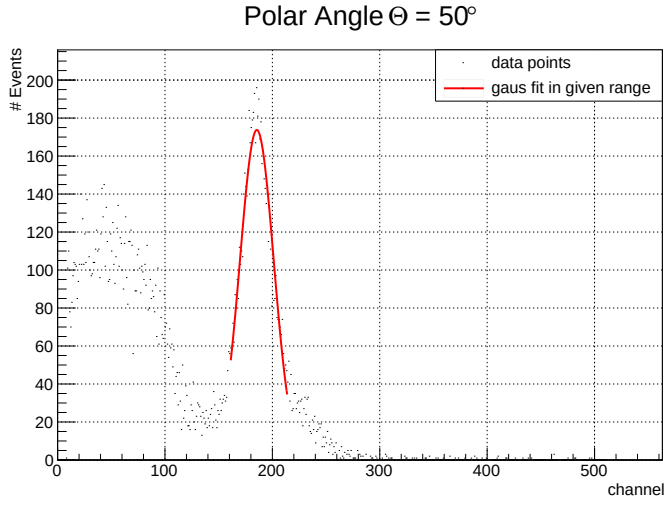

Figure 2.6: Fit to determine the energy at a fixed angle of $\Theta = 50°$.

Figure 2.7: Channels with errors given by gaussian fits and corresponding energies with errors for each angle Θ

Angle Θ in $^\circ$	Channel	Deviation	Energy in keV	σ_{Energy} in keV
20	92.79	9.28	35.18	159.30
30	104.78	11.40	78.83	163.04
40	119.50	12.34	132.45	166.58
50	138.39	14.43	201.24	172.56
60	160.93	16.72	283.35	180.28
70	185.53	15.68	372.96	185.20
80	211.99	17.88	469.33	195.06
90	237.73	19.34	563.07	204.51
100	261.00	20.08	647.80	212.75

As described in the preparation we have the equation

$$\frac{1}{E'} = \frac{1}{E} + \frac{1}{m_0 \cdot c^2} \cdot (1 - \cos\Theta)$$

So we plot the inverse energy $\frac{1}{E}$ over $1 - \cos(\Theta)$. The inverse of the slope gives then the invariant mass of the electron in keV. The resulting parameters are given by:

$$\text{y} - \text{intercept} = (1.20237 \pm 0.553517) \cdot 10^{-4}\ keV^{-1}$$

$$\text{slope} = (4.55878 \pm 3.02294) \cdot 10^{-3}\ keV^{-1}$$

As a result we can calculate the electron mass to be:

$$(219.357 \pm 145.456)\ keV$$

The results are not good which can be seen by comparing them with the values it should be, namely $m_e \approx 515\ keV$ and $(\text{y} - \text{intercept})^{-1} = E_{Cs_137} \approx 602\ keV$. The problem here is the big relative deviation of the inverse energies. To get better results we keep the y-intersect constant at the known $1/(602\ keV)$. The resulting plot is given in Fig.2.8, which looks in this scaling really similiar to the plot with variable intersect. The resulting parameter is:

$$slope = (2.59972 \pm 1.88442) \cdot 10^{-3}\ keV^{-1}$$

The final result for the electron mass is therefore:

$$m_e = (384.66 \pm 278.82)\ keV$$

The theoretical value of $m_e = 602\ keV$ lies withing one standard deviation of our result.

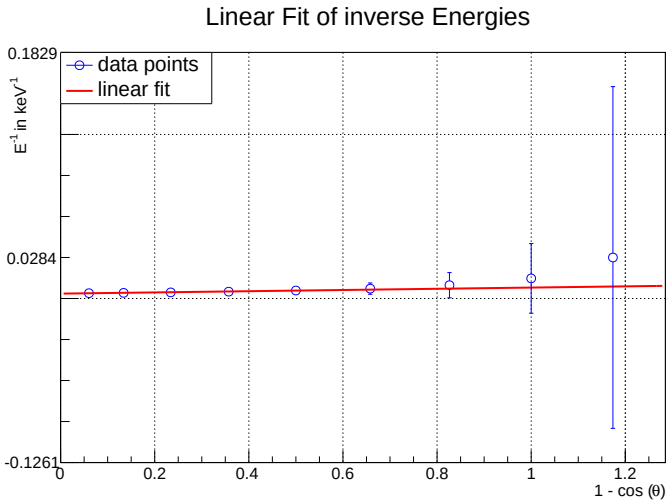

Figure 2.8: Fit to determine the invariant mass of electrons. The uncertainty is big for high values of $\frac{1}{E}$ due to the big uncertainty of the y-intercept in the calibration fit.

2.4 Cross Section for Different Materials

As described in the preparation the following formular should be true given that the binding energy is much smaller than the energy of the photons:

$$(\frac{\mathrm{d}\sigma}{\mathrm{d}\Omega})_e = const. \cdot R\frac{A}{\rho Z}$$

We measured the total number of events for a fixed angle $\Theta = 20°$ for different targets and subtracted the background $R = R_{target} - R_{background}$. The materials are aluminium, copper, iron and lead. Each target has the same size and shape.
To check the formular above we plot $\frac{R \cdot A}{\rho Z}$ over Z. This should be a horizontal line. Here A is the atomic mass, ρ is the density of the material and Z is the atomic number. The used values are given in Fig.2.9.

The resulting graph is shown in Fig.2.10. All data points except the one for lead are on a horizontal line. The reason is that the binding energy of lead is higher than for the others. Therefore the equation above doesn't hold true anymore because the electrons can't be simplified to be free anymore. It seems that with increasing atomic number, the error gets bigger.

Figure 2.9: Values used for the different materials in the equation above.

	aluminium	copper	iron	lead
ρ in $\frac{g}{cm^3}$	2.70	8.92	7.87	11.34
A in u	26.98	63.55	55.85	207.2
Z	13	29	26	82
R	19619	58964	55038	50573
$\sigma(R)$	1265.54	3688.28	3455.20	3477.25

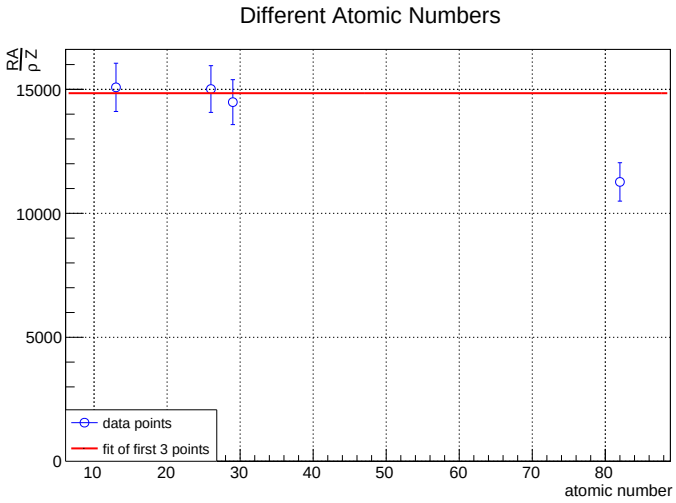

Figure 2.10: Plot of the quantity mentioned in the text over the atomic number Z with a fit of the first three data points. Lead doesn't align with the other materials. The reason is the binding energy of the electrons.

2.5 Conclusion

We calibrated the systems by calculating the corresponding energies for each channel. This was done by a linear fit. Our result cannot be compared with theoretical values, since it depends strongly on the experimental setup.
Next the differential cross section was calculated with respect to the solid angle Ω. Our results differ from the theoretical values given by the Klein-Nishina-Formular. The difference is bigger for larger angles. This seems to be a systematic uncertainty given by the experimental setup.
In the third paragraph the invariant mass of electrons was measured using the energy shift of the compton scattering. Here we had to use the theoretical value of the photons emitted by ^{137}Cs to get a reasonable result. Using this we found a good result. The theoretical value lies within one standard deviation of our calculated value.
Lastly we compared the cross section of different materials. For aluminium, copper and iron the results align reasonably well with our prediction. For lead the binding energy is too high and therefore the requirements are not fulfilled.